Virology 426 (2012) 42–50

Contents lists available at SciVerse ScienceDirect

Virology

journal homepage: www.elsevier.com/locate/yviro

A novel quadripartite dsRNA virus isolated from a phytopathogenic filamentous fungus, *Rosellinia necatrix*☆

Yu-Hsin Lin [a,1], Sotaro Chiba [a,1], Akio Tani [a], Hideki Kondo [a], Atsuko Sasaki [c], Satoko Kanematsu [b], Nobuhiro Suzuki [a,*]

[a] Institute of Plant Science and Resources, Okayama University, Kurashiki, Okayama 710-0046, Japan
[b] Apple Research Station, National Agricultural and Food Research Organization (NARO), 92 Shimokuriyagawa, Morioka, Iwate 020-0123, Japan
[c] National Institute of Fruit Tree Science, National Agricultural and Food Research Organization (NARO), 3 Fujimoto, Tsukuba, Ibaraki, 305-8605, Japan

ARTICLE INFO

Article history:
Received 31 October 2011
Returned to author for revision
5 December 2011
Accepted 14 January 2012
Available online 8 February 2012

Keywords:
Rosellinia necatrix
dsRNA
Mycovirus
Quadripartite genome
Virocontrol
White root rot
Quadrivirus

ABSTRACT

Here we report the biological and molecular attributes of a novel dsRNA virus isolated from *Rosellinia necatrix*, a filamentous phytopathogenic fungus. The virus, termed *Rosellinia necatrix* quadrivirus 1 (RnQV1), forms rigid spherical particles approximately 45 nm in diameter in infected mycelia. The particles contain 4 dsRNA segments, dsRNA1 to dsRNA4, with a size range of 4.9 to 3.7 kbp, each possessing a single large ORF. A comparison of the virus-infected and -cured isogenic fungal strains suggested that RnQV1 infection has no appreciable phenotypic effects. Phylogenetic analysis using the dsRNA3-encoded RdRp sequence revealed that RnQV1 is more distantly related to quadripartite chrysoviruses than to monopartite totiviruses, and is placed in a distinct group from other mycoviruses. No significant sequence similarities were evident between known proteins and RnQV1 structural proteins shown to be encoded by dsRNA2 or dsRNA4. These suggest that RnQV1 is a novel latent virus, belonging to a new family.

Introduction

Viruses are found in a wide range of major fungal groups (Ghabrial and Suzuki, 2009; Nuss, 2005; Pearson et al., 2009). Increasing numbers of novel fungal viruses (mycoviruses) are being reported from various host fungi (e.g., (Aoki et al., 2009; Cai et al., 2009; Chiba et al., 2009; Liu et al., 2009)). Mycoviruses are now classified into 11 families, including one (Megabirnaviridae) that is currently awaiting ratification by the International Committee on Taxonomy of Viruses (ICTV) (http://talk.ictvonline.org/default.aspx), and many that are still unassigned (Chiba et al., 2009; Ghabrial and Suzuki, 2009). Of these 11 families, 5—*Totiviridae*, *Partitiviridae*, *Chrysoviridae*, *Reoviridae*, and Megabirnaviridae—have double-stranded (ds) RNA genomes encapsidated by rigid virus particles, and their genome segment numbers are 1, 2, 4, 11 or 12, and 2, respectively. The remaining 6 families have single-stranded (ss) RNA genomes, many of which do not form virus particles. Members in the families *Totiviridae* and *Partitiviridae* are found frequently in fungi, while members of the remaining megabirnaviruses, chrysoviruses and reoviruses have been reported in a limited range of host fungi. Although many fungal viruses have no or few overt effects on their host fungi, some induce phenotypic alterations including hypovirulence (attenuated virulence) and debilitation on their hosts.

White root rot is one of the most destructive diseases in perennial crops worldwide particularly in fruit trees in Japan, caused by a soil-borne ascomycete *Rosellinia necatrix*. This fungus has attracted attention not only as an important plant pathogen but also as a host of viruses useful for studying virus/host and virus/virus interactions (Ghabrial and Suzuki, 2009). An extensive search of over 1000 field isolates for dsRNA has been conducted by N. Matsumoto and co-workers (Arakawa et al., 2002; Ikeda et al., 2004). Among their important findings, it has been shown that approximately 20% of *R. necatrix* fungal strains tested contain dsRNAs, considered to be mycovirus genomes or replication intermediates, and that the electropherotypes of the isolated dsRNAs vary, suggesting single and mixed infections by diverse viruses. To date, however, only a limited number of viruses have been characterized at the molecular and biological levels, e.g., members of the families *Reoviridae* (Wei et al.,

☆ The complete nucleotide sequences of dsRNA1 to dsRNA4 in this article have been deposited with the EMBL/GenBank/DDBJ Data Library under Accession Nos. AB620061 to AB620064.

* Corresponding author at: IPSR, Okayama University, Chuou 2-20-1, Kurashiki, Japan. Fax: +81 86 434 1232.
E-mail addresses: dns421461@s.okayama-u.ac.jp (Y.-H. Lin), chiba@rib.okayama-u.ac.jp (S. Chiba), atani@rib.okayama-u.ac.jp (A. Tani), hkondo@rib.okayama-u.ac.jp (H. Kondo), sasaatu@affrc.go.jp (A. Sasaki), satokok@affrc.go.jp (S. Kanematsu), nsuzuki@rib.okayama-u.ac.jp (N. Suzuki).

[1] These authors contributed equally to this work.

0042-6822/$ – see front matter © 2012 Elsevier Inc. All rights reserved.
doi:10.1016/j.virol.2012.01.013

2004), *Partitiviridae* (Sasaki et al., 2005), and Megabirnaviridae (Chiba et al., 2009).

Notably infection by Mycoreovirus 3 (MyRV3) (Kanematsu et al., 2004) or Rosellinia necatrix megabirnavirus 1(RnMBV1) (Chiba et al., 2009) alone has been shown to reduce the virulence and colony growth rate. A complex case of host fungal hypovirulence was assumed to result from mixed infection with *Rosellinia necatrix partitivirus 1* (RnPV1) and RnMBV2 (Sasaki et al., 2005; A. Sasaki, unpublished results). These findings have been obtained as a result of technical advances made in this host/virus system. For example, reproducible transfection protocols employing purified virus particles have been developed for members of the families *Reoviridae* (Sasaki et al., 2007), *Partitiviridae* (Sasaki et al., 2005), and Megabirnaviridae (Chiba et al., 2009). Virus curing by hyphal tipping and protoplast regeneration, and virus introduction between mycelially compatible fungal strains via hyphal anastomosis (Kanematsu et al., 2004) and mycelially incompatible fungal strains via protoplast fusion (A. Sasaki, unpublished results) can be achieved relatively easily. In addition, fungus transformation can be achieved with foreign genes (Kanematsu et al., 2004; Pliego et al., 2009). These available techniques have helped to clarify the cause–effect relationship of phenotypic alterations of fungal strains infected with viruses.

Here we determined the complete sequence of a novel virus observed in *R. necatrix* strain W1075 that had previously been isolated as a dsRNA-positive strain from Japanese pear in Japan. Moreover, we conducted analyses on the genome organization, virion structure, and phylogeny of the virus and tested its effect on the host phenotype.

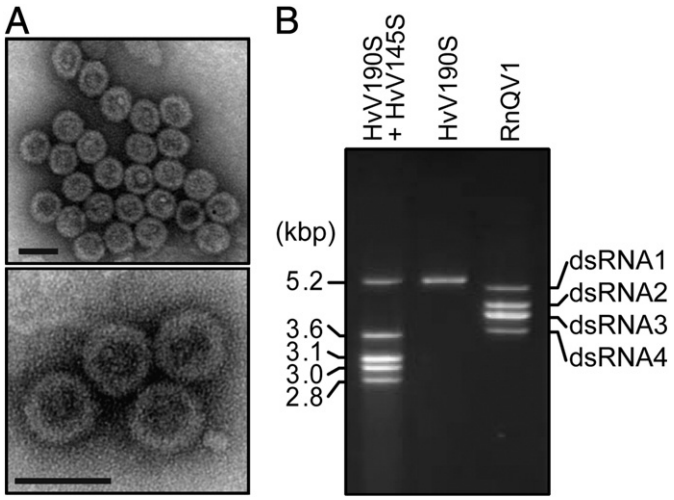

Fig. 1. RnQV1 particle morphology and RNA component. (A) Electron micrograph of RnQV1. Virus particles purified from fungal strain W1075, as described in Materials and methods, were examined using a Hitachi H-7650 electron microscope after negative staining with 2% uranyl acetate. Top and bottom panels are photographs of different enlargements. Bars indicate 50 nm. (B) Agarose gel electrophoresis profile of RnQV1 genomic dsRNA segments. RNA was isolated from purified RnQV1 preparations, and applied to lanes of 1.0% agarose gel. Electrophoresis was performed in 1× TAE (40 mM Tris-acetate, 1 mM EDTA, pH 7.8) at 50 V constant voltage for 4 h. RNA was stained with ethidium bromide. Genomic RNA segments of HvV190S (victorivirus) alone or together with HvV145S (chrysovirus), isolated from the virus-purified fraction (for HvV190S) or dsRNA fractions from *H. victoriae* mycelia of strain 83 coinfected with the two viruses (for HvV190S and HvV145S) were used as size standards.

Results

Biological comparison of virus-cured and -infected fungal strains

A total of 28 isolates were obtained by hyphal tipping and examined for the presence of dsRNA. Two of them, W1075-VF1 and W1075-VF2 were found to be virus-free by electrophoretic analysis of dsRNA (Fig. S1A) and Northern blotting (data not shown), and used subsequently as reference strains. The remaining isolates carried a set of four dsRNAs, showing the same dsRNA profile as the parental strain (data not shown).

The virus-infected W1075 and the two isogenic virus-cured isolates (W1075-VF1 and -VF2) were subjected to morphological comparison under different culture conditions. We measured the growth rates and observed the phenotypes of the three strains when cultured on potato dextrose agar (PDA) medium in the dark or under bench top conditions. No appreciable differences were detected under any condition (Fig. S1B).

Virulence assays with apple rootstocks were also performed. Both virus-infected (W1075) and isogenic virus-cured strains (W1075-VF1 and -VF2) penetrated the roots of apple rootstocks and killed them. No significant difference between these fungal strains was observed in terms of the number of dead plants 8 weeks after inoculation, or the severity of root disease (data not shown). Thus, the virus RnQV1 appeared to have little effect on the virulence level of the host fungus.

Virus particles and genomic dsRNAs

Purified virus particles had an icosahedral structure with rough surface when negatively stained using 2% uranyl acetate. The diameter of the particles was estimated to be approximately 45 nm (Fig. 1A). Most particles were penetrated by the stain, showing a donut appearance in contrast to RnMBV1 particles with no staining in the center (Chiba et al., 2009).

Purified preparations contained at least 4 dsRNA species that could be resolved in 1.0% agarose gel and were designated as dsRNA1 to dsRNA4 in an increasing order of mobility (Fig. 1B, lane RnQV1). The chemical nature of the dsRNA was confirmed by the ability to bind to CC41 cellulose and insusceptibility to DNase I and S1 nuclease (Fig. S1A). Despite a difference in size range, the agarose gel electrophoretic pattern of the dsRNAs was visually very similar to that of a member of the family *Chrysoviridae*, *Helminthosporium victoriae* virus *145S* (HvV145S) (Fig. 1B, lane HvV145S + HvV190SV), although they migrated between the largest segment (dsRNA1, 3.6 kbp) of HvV145S and the genome segment of a victorivirus *Helminthosporium victoriae* virus *190S* (HvV190S) (5.2 kbp). The sizes estimated for RnQV1 dsRNA1 to dsRNA4 by agarose gel analysis were 4.9, 4.5, 4.2 and 3.9 kbp. This dsRNA profile was identical when dsRNA fractions were obtained from purified particles and mycelia (Fig. 1, Fig. S1A). That is, the accumulations of dsRNA1 and dsRNA4 were consistently less than those of dsRNA2 and dsRNA3.

RNA sequences

A cDNA library for a mixture of dsRNAs 1 to 4 was constructed. The sizes of randomly selected cDNA clones were analyzed by agarose gel electrophoresis. As expected from size-based fractionation during the cDNA construction, the resulting cDNA clones contained inserts of over 1.5 kbp. A total of 41 clones were sequenced, and assembled into 5 contigs designated A to E of 3292, 1394, 4304, 3925 and 3343 nucleotides (nt). These five contigs were assigned to dsRNA segments by Northern blotting using representative cDNA fragments as probes (Fig. 2B). Each probe allowed the detection of a single dsRNA band, confirming that contigs A to E corresponded to dsRNA1, dsRNA1, dsRNA2, dsRNA3, and dsRNA4, respectively (Fig. 2). None of the clones formed separate contigs, suggestive of the absence of dsRNA other than dsRNA1 to dsRNA4. This notion was supported by PAGE analysis (data not shown). Based on the size estimation by agarose gel electrophoresis (Fig. 1B), contigs A to E were expected to span approximately 67%, 28%, 95%, 93% and 85% of the respective entire segments.

To determine the terminal sequences of dsRNA1 to dsRNA4, 3′-RLM-RACE (3′-RNA ligase mediated-rapid amplification of cDNA ends) was conducted in which an adaptor deoxyoligonucleotide was ligated to the 3′ end of each strand of the genomic RNAs. Amplified

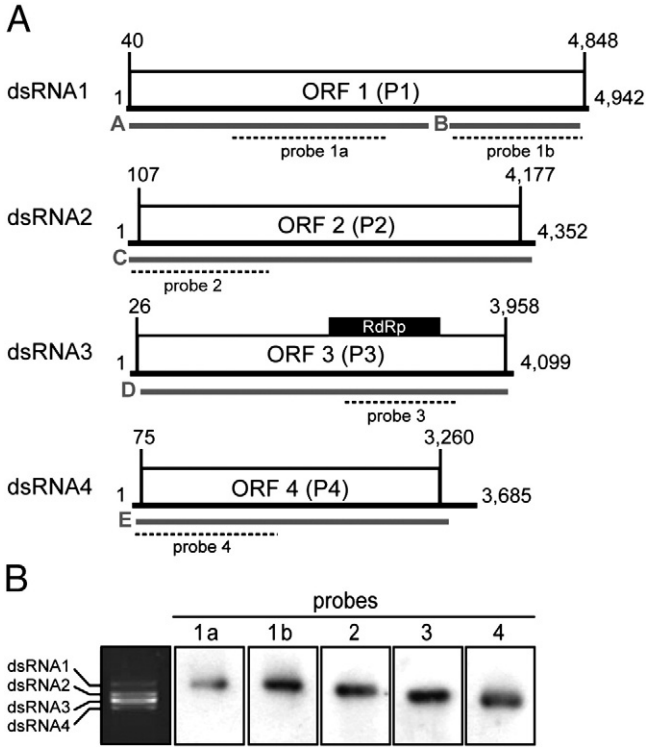

Fig. 2. Genetic organization and assignment of cDNA contigs of the RnQV1 genomic dsRNAs. (A) Schematic representation of the RnQV1 genomic segments. DsRNA1 to dsRNA4 are 4942, 4352, 4099, and 3685 bp in size. Each segment contains a relatively short 5′ and 3′ UTRs and a single large ORF shown by a box. The nucleotide positions of the initiation and termination codons and contigs A to E generated from the cDNA library are shown by numbers and solid bars above the ORFs and below the genome, respectively. Representative cDNA fragments indicated beneath the contigs by dashed line were used as probes in Northern analysis. (B) Northern blot analysis of RnQV1 genomic dsRNAs. Purified viral dsRNAs were separated in 0.7% agarose gel in 1× TAE, denatured, and blotted onto nylon membrane. Transferred RNAs were allowed to hybridize to each of the probes shown in A. Ethidium bromide-stained viral dsRNAs are shown on the left.

DNA fragments, shown by arrows in Fig. S2, were cloned and subjected to sequence analysis. At least 15 RLM-RACE clones were analyzed for each end of both the strands of dsRNA1 to dsRNA4 (Table S1). Regardless of which dsRNA was used as template, most or all 3′-RLM-RACE clones, corresponding to the 5′ terminus of the plus-sense strand had sequences 5′-$^{C}/_{U}$ACGAAU——, while those of the 3′ terminus of the plus-sense strand had sequences ——CAUGA-GAAUAUUC$^{G}/_{A}$-3′. Interestingly, the results of RLM-RACE summarized in Table S1 showed sequence heterogeneity at the extreme termini (5′-C/U———G/A-3′). To further confirm the variable end nucleotides, a circular RACE (c-RACE) was employed on dsRNA2 and dsRNA3. Consequently, the same heterogeneity was observed at the 5′ end of the plus strand of dsRNA3 and the 5′ termini of both strands of dsRNA2. It should be noted that the two RACE methods allow for sequence determination of the same ends using the different strands of a dsRNA segment.

Genetic organization of dsRNA1 to dsRNA4

The complete sequences of the genome segments were obtained from the contig sequences, gap-filling RT-PCR clones (between dsRNA1 contigs A and B), and RACE clones. Nucleotide sequences of single sites were confirmed by sequencing at least two cDNA clones from both directions. Sequence differences among cDNA clones, all being transitions, were found. For example, nucleotide substitutions at positions 3488 and 4637 on dsRNA1 and at positions 1044 on dsRNA2 were found. Completing the sequence of the genomic RNAs revealed a basic structure of genetic organization: each segment comprises a 25–106 nt 5′ untranslated region (UTR), a single large ORF corresponding to 86–97% of its entire size, and a 94–425 nt 3′ UTR. DsRNA1 to dsRNA4 encoded proteins named P1 (ORF1) to P4 (ORF4) of 1602 amino acids (aa), 1356 aa, 1310 aa and 1061 aa, respectively. A schematic representation of the genetic organization of dsRNA1 to dsRNA4 is shown in Fig. 2A. Some properties of the RnQV1 segments and representative dsRNA mycoviruses are summarized in Tables 1 and 2, respectively. It should be noted that the entire genome size of RnQV1 (17,078 bp, see Table 1 for the size of each segment) far exceeds that of any other mycoviruses with quadripartite genomes (Table 2), such as chrysoviruses (11,856–12,640 bp) (Covelli et al., 2004; Ghabrial, 2008; Jiang and Ghabrial, 2004) and AaV-1 (10,404 bp) (Aoki et al., 2009).

Each segment of RnQV1 has terminal sequence domains. The 5′ 7 nucleotides and 3′ 14 nucleotides (5′-$^{C}/_{U}$ACGAAU———CAUGA-GAAUAUUC$^{G}/_{A}$-3′) are conserved in the 4 dsRNA segments (Figs. 3A and B). Besides the strictly shared sequences, sequence stretches with high levels of similarity extend until position 32 for the 5′ termini and position 57 for the 3′ termini. An inverted repeat of 5 or 6 base pairs can potentially be formed by the strictly conserved terminal sequences of each segment (Fig. 3C). Two stem-loop structures can be formed by the sequence stretches adjacent to the strictly conserved 3′-terminal sequences of each segment (shown by two pairs of arrows in Fig. 3B). As is observed in all members of the family *Chrysoviridae* and some members of the *Partitiviridae* (Jiang and Ghabrial, 2004; Kozak, 1989; Tavantzis, 2008), "CAA" repeats, presumably serving as a translational enhancer, were found on dsRNA1, dsRNA2, and dsRNA4 within the 5′ UTR and coding region (Fig. 3A). It is interesting to note that dsRNA3 possesses neither typical CAA repeats nor a strong AUG codon according to Kozak's rule (Kozak, 1989). This suggests that dsRNA3-coded transcripts have a low level of translation activity. Similarly, HvV145S dsRNA1 has no typical CAA repeats (Ghabrial et al., 2002).

Assignment of the structural protein genes

SDS-PAGE analysis showed that purified particle preparations contained a few major proteins of 110, 100 and 75 kDa, along with minor proteins of 60 and 40 kDa (Fig. 4, lane VP). These protein bands were not found in preparations derived from the virus-free isogenic fungal strain, W1075-VF1 by the same method as that used for virus-infected W1075 (Fig. 4, lane VF). However, some minor bands

Table 1
Properties of the dsRNA segments of RnQV1.

Segment	Accession no.	ORF size (aa, kDa)	Putative function	Non-coding region length (nt)	
				5′-end	3′-end
dsRNA1 (4942 bp)	AB620061	4809 (1602 aa, 178.2)	Unknown[a]	39	94
dsRNA2 (4352 bp)	AB620062	4071 (1356 aa, 147.4)	Structural protein	106	175
dsRNA3 (4099 bp)	AB620063	3933 (1310 aa, 146.8)	RdRp	25	141
dsRNA4 (3685 bp)	AB620064	3186 (1061 aa, 113.2)	Structural protein	74	425

[a] Similar to hypothetical proteins encoded by the Amasya cherry disease-associated L dsRNA1 and dsRNA2 (CAJ29960, CAJ29961).

Table 2
Comparison between RnQV1 and other representative dsRNA mycoviruses.

Type species (genus, family)[a]	Genome segments		Coding strategy	Virion morphology (nm in diameter)	Major SP[b]	3′-poly (A)
	Number	Size range (total size)				
RnQV1 (Quadrivirus, Quadriviridae)	4	3.7–4.9 (17.1) kbp	Monocistronic	Isometric (~45)	≧2	Not found
HvV190S (*Victorivirus, Totiviridae*)	1	5.2 (5.2) kbp	Polycistronic	Isometric (33–40)	1	Not found
AaV-1 (Unassigned)	4	1.4–3.6 (10.4) kbp	Monocistronic	Isometric (33)	1	33–50 nt
PcV (*Chrysovirus, Chrysoviridae*)	4	2.9–3.6 (12.6) kbp	Monocistronic	Isometric (35–40)	1	Not found
RnMBV1 (Megabirnavirus, Megabirnaviridae)	2	7.2, 8.9 (16.1) kbp	Polycistronic?	Isometric (50)	1	Not found
AhV (*Partitivirus, Partitiviridae*)	2	2.1, 2.2 (4.3) kbp	Monocistronic	Isometric (30–35)	1	21–58 nt[c]
MyRV1 (*Mycoreovirus, Reoviridae*)	11	0.7–4.1 (23.4) kbp	Monocistronic	Isometric (80)	≧2	Not found

[a] Data are from Huang and Ghabrial (1996), Aoki et al. (2009), Jiang and Ghabrial (2004), Chiba et al. (2009), Oh and Hillman (1995), Hillman et al. (2004), and Suzuki et al. (2004). See the legend of Fig. 5 for non-abbreviated virus names except for *Atkinsonella hypoxylon virus* (AhV).
[b] SP: structural protein.
[c] Interrupted poly (A) stretch.

at 150, 135, 65 and 55 kDa (shown by asterisks) were detected commonly in lanes VP and VF (Fig. 4). These appeared to be host proteins cofractionated with the virus particles. Minor proteins of 37 and 30 kDa were occasionally observed whose detection levels varied between virus particle preparations (data not shown).

The proteins of 110, 100, 75, 60 and 40 kDa (Fig. 4) were subjected to peptide mass fingerprinting (PMF) and subsequent MS/MS analysis to identify their corresponding genes. Based on molecular mass calculations, sequences were obtained for a number of peptide fragments derived from trypsin digestion, and the analyzed proteins were identified as being of either P2 or P4 origin (Fig. 4, Table S2). For example, the sequences inferred from molecular masses of 8 tryptic peptides of the 110-kDa protein were all observed in the amino acid sequences (P4) deduced from the nucleotide sequences of the RnQV1 dsRNA4 (Tables S2 and S3). Some tryptic peptides analyzed by MS/MS analysis confirmed their coding segment. Likewise, it was shown that the 100-, 75-, 60-, and 40-kDa polypeptides were encoded by dsRNA2, dsRNA4, dsRNA2, and dsRNA2, respectively (Fig. 4, Tables S2 and S3). These conclusions were supported by MOWSE (MOlecular Weight SEarch) scores higher than 19 ($p<0.05$) (Fig. 4, Table S2). SDS-PAGE-based size estimation (Fig. 4, left panel) and peptide sequence distribution profiles allowed for the prediction of the corresponding portions of the structural proteins as shown by light green and violet areas (Fig. 4, right panel). No significant hit was yielded by PMF of the proteins denoted by asterisks, supporting their host origin.

Amino acid sequence similarities and phylogenetic analysis

Before describing the relationship of RnQV1 with other viruses, Amasya cherry disease (ACD)- and cherry chlorotic rusty spot (CCRS)-associated dsRNAs and mycovirus genome-like sequence termed grapevine associated totivirus 1 (GaTV-1) should be explained briefly (Al Rwahnih et al., 2011; Covelli et al., 2004). ACD and CCRS occurring in Turkey and Italy, are suspected to have a fungal etiology, although no definitive conclusion has yet been reached. Diseased plants show a complex profile of 10 to 12 dsRNA elements (Covelli et al., 2004). Among them are ACD and CCRS L dsRNA1 to L dsRNA4 with a size range of 5121 to 4303, which are two RdRp-coding segments and two of RnQV1 dsRNA1-related segments (Kozlakidis et al., 2006). Therefore, those dsRNA elements appear to represent the genomes of two related viruses. However, whether the viruses are of plant or fungal origin and whether it forms particles in infected cells are unclear. The GaTV-1 sequence was assembled from deep sequencing reads derived from a PCR-based cDNA library of dsRNAs extracted from a single grapevine.

The results of a BLAST search with RnQV1 P3 (RdRp) are summarized in Table S4. The BLAST search showed that P3 shares 20–31% amino acid sequence identity to RdRps from other mycoviruses within the families *Totiviridae*, *Chrysoviridae* and Megabirnaviridae (see Fig. S3 for an alignment of RdRp domains). Highest BIT scores (211–631) and identities (35–41%) were found between RnQV1 P3 and RdRp encoded by ACD L dsRNA3 and L dsRNA4, and CCRS L

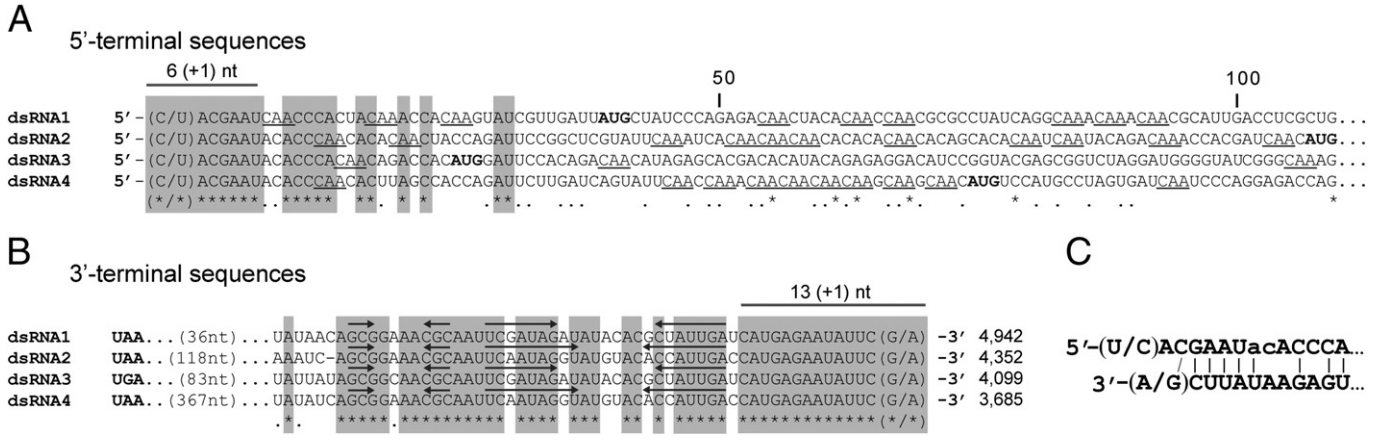

Fig. 3. Terminal sequence domains of the RnQV1 genome. (A, B) Sequences of the 5′ (A) and 3′ termini (B). The 7 5′-terminal nucleotides, 14 3′-terminal nucleotides and some sequence stretches shared by the four segments are shaded, while the extreme termini show variability (5′-C/U————G/A-3′). CAA repeats in the 5′ terminal region are underlined, and the possible initiation codons AUGs and termination codons UAA or UGA are shown in bold. Two stem-loop structures could be generated on each segment by the conserved sequences denoted by arrows. (C) An inverted repeat formed by the strictly conserved terminal sequences. A 5 to 6 base-pairing could be formed by the 5′ and 3′ conserved terminal sequences (shown by solid lines above the sequences in A and B) of each segment. Note that dsRNA1 has a dinucleotide (CA) in place of AC at positions 8–9 which is shown as lowercase letters (ac).

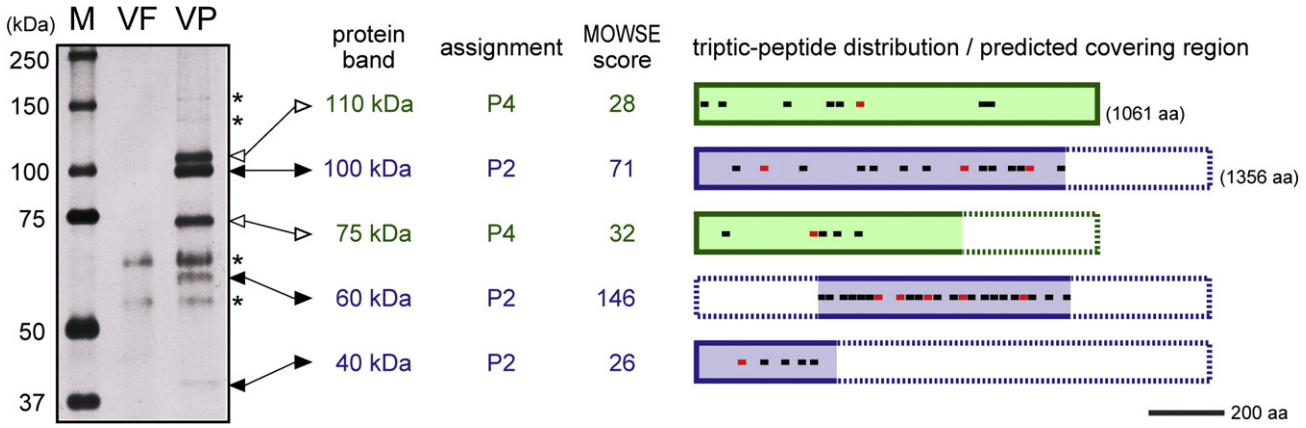

Fig. 4. Genome segment assignment of RnQV1 structural proteins. SDS-polyacrylamide gel and analysis of purified virus preparations. Purified virus particles (VP) were denatured in the presence of SDS and β-mercaptoethanol for 5 min at 95 °C, and electrophoresed in 10% polyacrylamide gel. Protein preparations obtained from virus-free fungal strain W1075-VF1 (VF) by the same method as that used for W1075 were treated in parallel. Proteins were visualized with silver staining. M refers to the prestained protein size standards from Bio-Rad (Precision Plus Protein Standards). Polypeptides denoted by solid and clear arrowheads were shown by PMF and MS/MS analyses to be encoded by dsRNA2 and 4, respectively (see Table S2). Proteins marked by asterisks were detected commonly in preparations obtained from virus-free mycelia (unknown host protein). Peptide mass fingerprinting (PMF) and MS/MS analyses of RnQV1 structural proteins. Proteins of 110, 100, 75, 60, and 40 kDa in RnQV1 purified preparations (see Fig. 4, left panel) were analyzed as described in Materials and methods. Tryptic peptides, whose sequences were determined (see Table S3), were mapped on the amino acid sequences deduced from the nucleotide sequences of the dsRNA2 (P2) and dsRNA4 ORFs (P4) on the right. MOWSE scores are shown in the middle for each polypeptide. MOWSE scores greater than 19 are significant ($p<0.05$). Red bars indicate peptide fragments analyzed by MS/MS, while black bars refer to those analyzed by PMF. The polypeptides of 110 and 75 kDa, and 100, 60, and 40 kDa are predicted to correspond to P4 and P2 portions colored by light green and violet, respectively.

dsRNA3 and L dsRNA4. The protein encoded by RnQV1 dsRNA1 (P1) showed, albeit within a limited region (overlaps: 489 and 156 aa), low levels of sequence similarity (19% and 27% identity) to uncharacterized proteins encoded by ACD L dsRNA1 and L dsRNA2 and GaTV-1 (Al Rwahnih et al., 2011; Covelli et al., 2004). It should be noted that these four proteins showed similar secondary structure profiles (Fig. S4) when predicted by a bioinformatic tool FoldIndex (Prilusky et al., 2005) (http://bip.weizmann.ac.il/fldbin/findex#info) (Fig. S4). Proteins encoded by dsRNA2 and dsRNA4 (P2 and P4), identified as structural proteins by previous experiments, did not provide any significant hit against the protein databases. A pfam search with RnQV1 P1 to P4 revealed that P3 belongs to the viral RdRp family (RdRp_4), but no significant hit was found in P1, P2, or P4. No motif or pattern was found in those proteins by a PROSITE database search with default settings that excluded those frequently found.

Sequences of RdRp from fungal-, protozoa-, and arthropod-infecting dsRNA viruses and dsRNA elements were aligned using the MAFFT program, and refined the alignment by removal of gaps in MEGA4 (Fig. S3). The mid-point rooting maximum-likelihood (ML) dendrogram was generated based on the refined alignment with the appropriate setting for the tree construction. As shown in Fig. 5, the tree placed RnQV1 P3 together with RdRps encoded by ACD L dsRNA3, L dsRNA4 and CCRS L dsRNA4 in a separate clade distinct from other reported mycoviruses including the definitive members of the quadripartite *Chrysoviridae* family.

Discussion

A growing number of novel mycoviruses have been reported recently. Characterization of these viruses has enhanced our understanding of the molecular evolution and diversity of viruses, and led to the discoveries of novel virion structures and genome organizations (Aoki et al., 2009; Cai et al., 2009; Chiba et al., 2009; Ghabrial and Suzuki, 2009; Jamal et al., 2010; Liu et al., 2009; Urayama et al., 2010). This study investigated the morphological and molecular properties of another novel dsRNA virus with a quadripartite genome, designated as Rosellinia necatrix quadrivirus 1 (RnQV1), isolated from the white root fungus. The novelty of RnQV1 can be readily appreciated in the lack of significant sequence similarity between P2 or P4 and known protein sequences, and the limited sequence similarities of RnQV1 P1 to proteins encoded by ACD-associated L dsRNA1 and dsRNA2, and of RnQV1 P3 to RdRps from other established mycoviruses (Table 2). The quadripartite nature of the RnQV1 genome (dsRNA1 to dsRNA4) was verified by several observations. Purified preparations of spherical virus particles approximately 45 nm in diameter contained all four dsRNA segments and dsRNA2- and 4-encoded proteins P2 and P4 (Figs. 1, 2 and 4). The four segments share conserved terminal sequences (Fig. 3). All hyphal-tip fungal isolates carried all (26 isolates) or none (2 isolates) of the four dsRNA segments, indicating transmission of the four segments in an all-or-none fashion (Fig. S1). Furthermore, only one of the segments, dsRNA3, encodes RdRp. These findings strongly support the quadripartite nature of RnQV1.

RnQV1 is reminiscent of members of the family *Chrysoviridae*, although it is readily distinguished from other dsRNA mycoviruses (Table 2). The family *Chrysoviridae* is a relatively new and small virus family, containing two definitive fungal virus members, *Penicillium chrysogenum* virus (PcV) and HvV145S, and a few tentative members (Ghabrial, 2008). Similarities between RnQV1 and chrysoviruses include the genome segment number 4, the electropherotype of the segments (compare Fig. 1B lanes HvV190S + HvV145S vs. RnQV1), the monocistronic nature of each segment, presence of the presumed translation enhancer represented by CAA repeats on the 5′ UTRs or within the adjacent coding region of the segments (Fig. 3A). However, two groups can be differentiated from each other. The whole genome size is 11.8 to 12.6 kbp for chrysoviruses and 17.1 kbp for RnQV1, being approximately 1.5-fold greater in the latter. RnQV1 particles are composed of more than two major structural proteins encoded by dsRNA2 and dsRNA4 (Fig. 1B, Table 1), while chrysovirus genomes are encapsidated by the single coat protein (CP) encoded by dsRNA2 (Jiang and Ghabrial, 2004). The terminal sequence domains of chrysoviruses consist of three elements, the extremely terminal sequence of approximately 3 to 10 nt strictly conserved among the four genomic segments, the adjacent well-conserved region termed Box 1 of approximately 50 nt, and the 7 to 11 CAA repeats (for PcV) (Jiang and Ghabrial, 2004). The CAA repeats of chrysoviruses are situated between the 5′ UTR region downstream of Box 1 and upstream of the translation initiation site, while those of RnQV1 are located in the 5′ UTR (dsRNA2 and dsRNA4) or both the 5′

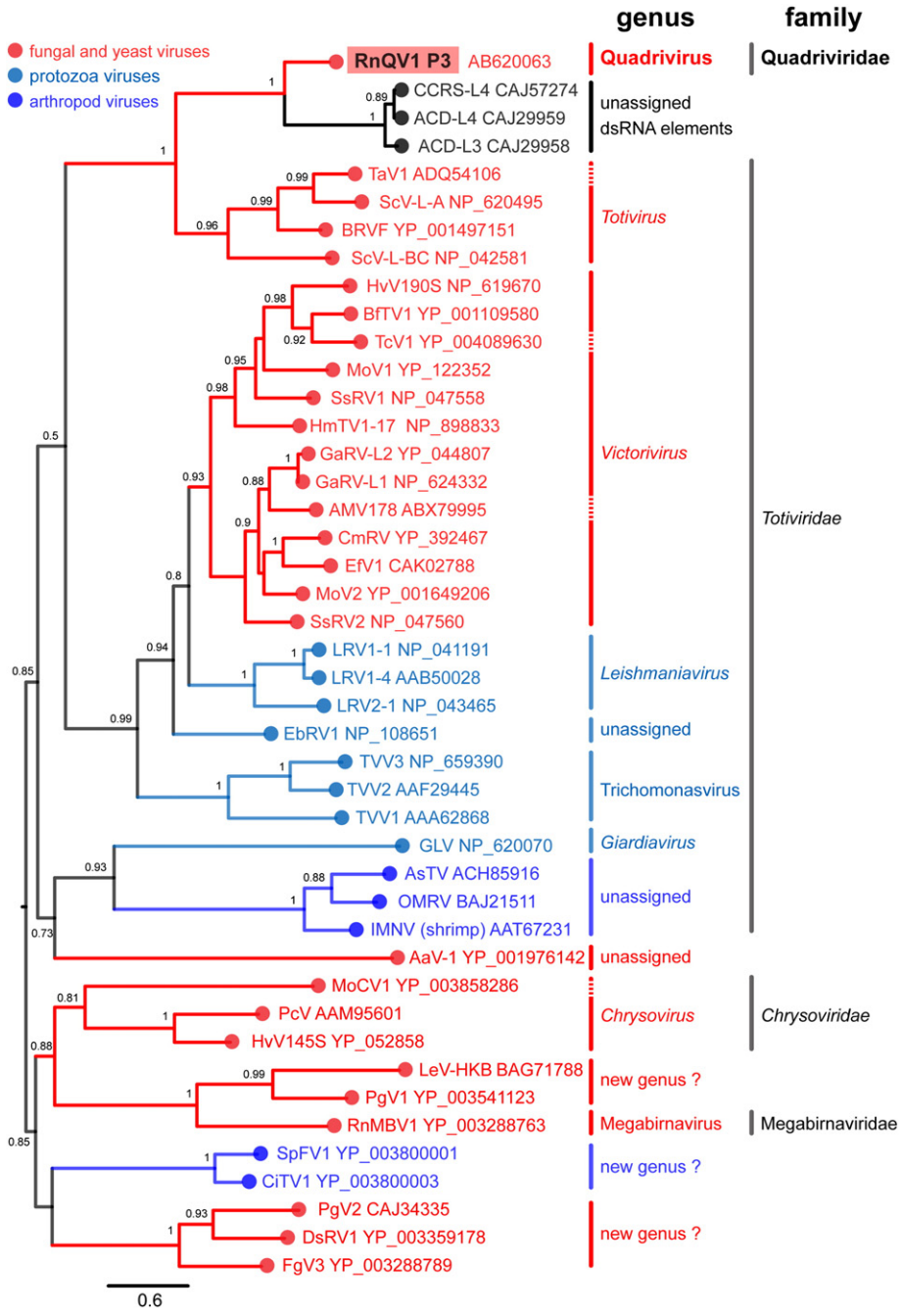

Fig. 5. Phylogenetic analysis of RnQV1. A phylogenetic tree was created based on the RdRp alignment that included representative members of fungal-, protozoa-, and arthropod-infecting dsRNA viruses and dsRNA elements. Definitive (in italics) and tentative (non-italics) virus genera and families are indicated by solid vertical lines. Dashed lines refer to dsRNA elements that are not recognized as virus species by the ICTV but closely associated with members of the virus families being proposed. Numbers at the nodes denote approximate likelihood ratio test (aLRT) values supporting reliability of branches. The scale bar represents the amino acid distances. Abbreviated names of viruses and dsRNA elements: CCRS-L4, cherry chlorotic rusty spot associated L dsRNA4; ACD-L3 and -L4, Amasya cherry disease-associated L dsRNA3 and L dsRNA4; TaV1, Tuber aestivum virus 1; ScV-L-A, *Saccharomyces cerevisiae virus L-A* (L1); BRVF, Black raspberry virus F; ScV-L-BC, *Saccharomyces cerevisiae virus L-BC*; HvV190S, *Helminthosporium victoriae virus 190S*; BfTV1, Botryotinia fuckeliana totivirus 1; TcV1, Tolypocladium cylindrosporum virus 1; MoV1 and MoV2, *Magnaporthe oryzae virus 1* and 2; SsRV1 and SsRV2, *Sphaeropsis sapinea RNA virus 1 and 2*; HmTV1-17, *Helicobasidium mompa totivirus 1–17*; GaRV-L1, *Gremmeniella abetina RNA virus L1*; GaRV-L2, Gremmeniella abietina RNA virus L2; AMV178, Aspergillus mycovirus 178; CmRV, *Coniothyrium minitans RNA virus*; EfV1, *Epichloe festucae virus 1*; LRV1-1, LRV1-4 and LRV2-1, *Leishmania RNA virus 1–1, 1–4* and *2–1*; EbRV1, Eimeria brunetti RNA virus 1; TvV1, TvV2 and TvV3, Trichomonas vaginalis virus 1, 2 and 3; GLV, *Giardia lamblia virus*; AsTV, Armigeres subalbatus virus SaX06-AK20; OMRV, Omono River virus AK4; IMNV, Penaeid shrimp infectious myonecrosis virus; AaV-1, Alternaria alternata virus-1; MoCV1, Magnaporthe oryzae chrysovirus 1; PcV, *Penicillium chrysogenum virus*; HvV145S, *Helminthosporium victoriae virus 145S*; LeV-HKB, Lentinula edodes mycovirus; PgV1, Phlebiopsis gigantea mycovirus dsRNA 1; RnMBV1, *Rosellinia necatrix* megabirnavirus 1/W779; SpFV1, Spissistilus festinus virus 1; CiTV1, Circulifer tenellus virus 1; PgV2, Phlebiopsis gigantea mycovirus dsRNA 2; DsRV1, Diplodia scrobiculata RNA1; FgV3, Fusarium graminearum dsRNA mycovirus-3.

UTR and coding domain (dsRNA1 and dsRNA3). The CP sequence and two other proteins encoded by the chrysovirus genomes show moderate similarities among definitive and tentative members. However, while the RdRp encoded by RnQV1 dsRNA3 show low levels (20–25% for the region spanning the conserved motifs) of similarity to those of chrysoviruses, no significant similarities are evident between the proteins encoded by dsRNA1, dsRNA2 or dsRNA4 and any chrysovirus-coded proteins. Recent structural analysis has shown that a

chrysovirus has a unique structure with a T = 1 lattice composed of the 60 CP subunit monomers each containing two duplicated domains (Caston et al., 2003). Morphological features of RnQV1, currently being investigated by cryo-electron microscopy combined with the 3D reconstruction method (S. A. Ghabrial, personal communication), will give a clearer picture of the taxonomical relationship between RnQV1 and the family *Chrysoviridae*.

The phylogenetic analysis with RdRp sequences placed RnQV1 along with ACD L dsRNA 3 and 4 in a different clade from other mycoviruses reported to date, as supported by a high aLRT value (Fig. 5). The close relationship is supported by their conserved 5′-terminal sequence (5′-UACGA——) (Fig. 3A), and aa sequence similarities between RdRps encoded by RnQV1 dsRNA3 and ACD L dsRNA3 (identity: 35%) or 4 (identity: 36%), and those between polypeptides encoded by RnQV1 dsRNA1 and ACD L dsRNA1 (identity: 19%) or 2 (identity: 27%). Similar relation is found between the RnQV1 genome segments and CCRS L dsRNA1 to L dsRNA4. A rooted phylogenetic tree was independently generated using the neighbor-joining method in which amino acid sequences flanking RdRp motifs III to VIII in Fig. S3 were analyzed by Clustal-X software. The tree topology was very similar to that of the ML dendrogram (Fig. 5, data not shown). It was slightly surprising that despite the similar features discussed above, RnQV1 and quadripartite chrysoviruses or AaV-1 are more distantly related than are RnQV1 and ACD L dsRNAs or *Totiviridae* (with monopartite genomes). Accordingly we propose the creation of a new genus (Quadrivirus) and family (Quadriviridae) to accommodate RnQV1 as the type species.

RnQV1 has two features distinguishing it from most other mycoviruses. Firstly, heterogeneity is evident at the terminal ends of each genome segment (5′-C/U———G/A-3′). RLM-RACE and c-RACE revealed greater frequencies of clones with Cs and Gs at the 5′ and 3′ ends, corresponding to the plus strand of a genome segment, than those with Ts and As. Based on their ratios shown in Table S1, the plus strand of each genome segment appears to be 5′-C———G-3′ or 5′-U—————A-3′. The terminal sequences of an RNA viral genome are generally believed to be important for RNA replication and packaging, and are usually strictly conserved. The terminal sequence variability was thus surprising. The heterogeneity is highly unlikely to have resulted from experimental artifacts or errors, because the terminal sequences of a novel partitivirus and a megabirnavirus from *R. necatrix* determined by the same methods as those used for RnQV1 in parallel showed homogeneity as reported by Chiba et al. (2009, 2011). It should be noted that both ends of the RNA genomes of a mitovirus, *Gremmeniella abietina* mitochondrial RNA virus S1 and a leishmaniavirus, Leishmania RNA virus 1 were reported previously to show extensive variations in sequence and length (Stuart et al., 1992; Tuomivirta and Hantula, 2003). Secondly, RnQV1 has multiple structural proteins encoded by dsRNA2 and dsRNA4, a rare feature for mycoviruses that are composed of single major CPs, except for double-shelled mycoreoviruses (Table 2). The expected sizes of P2 and P4 are 147 kDa and 113 kDa, respectively. PMF and MS/MS analyses suggest that the 110-kDa and 75-kDa proteins shown in Fig. 4 are likely to correspond to full-length P4 and its N-terminal two-thirds, respectively. The 60- and 40-kDa proteins likely correspond to the central and N-terminal portions of the 100-kDa protein, which is considered to originate from P2. It is unknown how the protein components in virus-purified preparations arise during the virus replication and/or purification procedure.

It is well established that the chestnut blight fungus, *Cryphonectria parasitica* supports replication of various viruses and has served as an amenable system for studies of virus/virus and virus/host interactions (Faruk et al., 2008; Hillman and Suzuki, 2004; Nuss, 2005, 2011; Segers et al., 2007; Sun and Suzuki, 2008; Sun et al., 2006). *R. necatrix* is also emerging as another versatile system suitable for mycovirus research based on the availability of basic techniques. An increasing number of viruses have been isolated in the white root rot fungus that are placed in one tentative and three established families: Megabirnaviridae, *Reoviridae, Partitiviridae*, and *Totiviridae*. These viruses show distinct pathogenicity, distribution patterns within fungal colonies, and particle morphology (Chiba et al., 2009; Kanematsu et al., 2004; Sasaki et al., 2005; Yaegashi et al., 2010). RnQV1 seems to be prevailing in this fungus, as a report by Arakawa et al. (2002) has described field isolates with dsRNA gel profiles similar to that of RnQV1 (compare Fig. 1B of the present article to Fig. 1b of the Arakawa et al. (2002)). Thus, the present study has provided an additional new virus species with distinct properties that may place it in a possibly novel virus family. The current characterization of RnQV1 will also provide molecular tools for exploring the complex nature of infections of the white root rot fungus by diverse viruses (Arakawa et al., 2002) and for studying dynamic interactions between viruses and between viruses and the host fungus.

Materials and methods

Fungal strains and culturing

R. necatrix strain W1075 was originally collected by Dr N. Matsumoto's group in 1997 from an orchard of Japanese pear in Saga Prefecture, Japan (S. Kanematsu and N. Matsumoto, unpublished results). W1075 belongs to the mycelial compatibility group 80 (MCG80) (Aimi et al., 2002). Single asexual spore isolation, often used to obtain virus-free isolates for filamentous fungi, is not applicable to *R. necatrix*, because it rarely develops germlings under laboratory conditions (Nakamura et al., 2002). In this study, two virus-cured isogenic strains designated as W1075-VF1 and W1075-VF2 were obtained from W1075 by hyphal tipping.

Helminthosporium victoriae strain 83 (ATCC 42018), provided by Dr Said A. Ghabrial (University of Kentucky), is coinfected with the type species of the genus *Victorivirus* of the family *Totiviridae*, HvV190S and a member of the family *Chrysoviridae*, HvV145S (Sanderlin and Ghabrial, 1978). Their genomic dsRNAs were used as size markers.

All fungal strains were grown at 22–25 °C in the dark or under bench top conditions on Difco™ PDA (Becton Dickinson, Sparks, MD, USA) for phenotypic observation, and in Difco™ potato dextrose broth (PDB) for virus purification and nucleic acid extraction, unless otherwise specified. Growth rates were assessed by measuring diameters of colonies 3, 6 and 9 days postinoculation in which five PDA plates were inoculated by each strain. The fungal strain was stored at −80 °C in the form of mycelia in 10% glycerol, and revived when necessary.

For virulence assay, ten apple rootstocks (*Malus prunifolia* var. ringo) were inoculated with freshly grown mycelia of the virus-infected (W1075) or -uninfected fungal strains (W1075-VF1 and W1075-VF2) and kept in a greenhouse at approximately 25 °C, as described by Kanematsu et al. (2004). Inoculated plants were monitored for 2 months and those showing lethal phenotype were scored on a weekly basis.

Virus purification and electron microscopy

Virus particles were purified as described by Sanderlin and Ghabrial (1978) with modification. Mycelia of fungal strain W1075 cultured in 3 l of PDB were harvested, and then ground to powder in the presence of liquid nitrogen. The homogenates were mixed with extraction buffer (0.1 M sodium phosphate, pH 7.0 containing 0.1% β-mercaptoethanol), and clarified with carbon tetrachloride. The virus-containing solution was subjected to differential centrifugation and subsequent sucrose density gradient (10% to 40%) centrifugation at 70,000×*g* for 2 h. A virus-containing zone located at a sucrose concentration of approximately 30% was further centrifuged

to sediment the particles, and then resuspended in 100 μl of 0.05 M sodium phosphate buffer, pH 7.0.

The virus preparation was examined under a Hitachi H-7650 electron microscope (Tokyo, Japan) after staining with 2% uranyl acetate.

cDNA cloning

DsRNA was extracted from 100 ml of a PDB culture by the method of Sun and Suzuki (2008) employing CC41 cellulose column chromatography. SsRNA and dsDNA were completely digested with S1 nuclease and subsequently with DNase I, as described by Suzuki et al. (2003). A cDNA library was generated as described by Chiba et al. (2009) using a Takara cDNA synthesis kit (Takara, Kyoto, Japan). Purified dsRNA fractions containing all the 4 segments were denatured in 90% dimethyl sulfoxide (DMSO) at 65 °C for 15 min (Asamizu et al., 1985) in the presence of random hexadeoxinucleotide, and reverse transcribed at 42 °C by moloney murine leukemia virus (MMLV) reverse transcriptase (Takara). An A residue was added to the resulting ds-cDNA using Taq DNA polymerase at 72 °C for 30 min, and the modified cDNA was electrophoresed for size fractionation. Gel-isolated cDNA of over 2 kbp was ligated with pGEM-T Easy (Promega, Fitchburg, WI, USA) and transformed into *Escherichia coli* strain DH5α.

RACE (rapid amplification of cDNA ends) analysis

Two RACE methods were used to determine the terminal sequences of dsRNAs. RNA ligase mediated RACE (RLM-RACE) was performed according to the method of Suzuki et al. (2004). A 5′-phosphorylated oligodeoxynucleotide (5′-PO_4-CAATACCTTCTGACCATG-CAGTGACAGTCAGCATG-3′) (3RACE-adaptor) was ligated to each of the 3′-termini of the four viral segments with T4 RNA ligase (Takara) in the presence of RNase inhibitor (Toyobo, Osaka, Japan) after denatured in 90% DMSO as described above. The ligates were used as templates for cDNA synthesis using MMLV reverse transcriptase (Invitrogen, Carlsbad, CA, USA), in which 3RACE-1st complementary to the 3′-half of the 3RACE-adaptor served as a primer. The resulting cDNA was amplified by PCR with the primer set, 3RACE-2nd (Table S5) complementary to the 5′-half of the 3RACE-adaptor and gene specific primers. A total of 8 PCR reaction products for both strands of the 4 segments were cloned into pGEM-T Easy for sequence analysis. A circular RACE (c-RACE) technique (Kondo et al., 2006) was also used to determine the terminal sequences of some dsRNA segments. For example, complementary DNA was synthesized using a 5′-phosphorylated oligonucleotide corresponding to map positions 748–770 of dsRNA2 (R2-5CD1) (Table S1). The resulting ss-cDNA was circularized or concatemerized by T4 RNA ligase. DNA fragments covering the ligated junction were amplified by PCR using a primer pair (R2-5FW2 and R2-5 CD3) (Table S5).

RNA extraction and Northern blot analysis

RNA was isolated according to the method of Suzuki et al. (2003). Briefly, total nucleic acids were purified by homogenizing mycelia in the presence of liquid nitrogen, two rounds of extraction with phenol/chloroform, chloroform-isoamyl alcohol and subsequent ethanol-precipitation. The resulting nucleic acids were treated with RNase-free DNase I (Promega). RNA was extracted from purified virus fractions by an SDS-phenol method (Chiba et al., 2009). Northern blotting, as described by Sun and Suzuki (2008), was performed using non-radio isotope probes, digoxigenin (DIG)-11-dUTP-labeled DNA fragments according to the method recommended by the manufacturer (Roche Diagnostics, Mannheim).

Sequence analysis and bioinformatics analysis

cDNA plasmid clones were sent to Macrogen Japan, Inc., (Tokyo) for sequencing, or sequenced using an ABI3100 DNA sequencer (Applied Biosystems, Foster City, CA, USA). The sequences were assembled and analyzed using the DNA processing software packages, AutoAssembler (Applied Biosystems) and GENETYX (SDC, Tokyo, Japan). A sequence similarity search was conducted with the BLAST program available from the National Center for Biotechnology Information (NCBI) (Altschul et al., 1997). A functional motif search was carried out against the Pfam database (Finn et al., 2008) and PROSITE database at http://prosite.expasy.org/. Multiple sequence alignments of RdRps were generated using the MAFFT program (Katoh and Toh, 2008) and refined in MEGA4 software (Tamura et al., 2007) by removing gaps manually (Fig. S3, highlighted region). The data set was subjected to Akaike's information criterion (AIC) for selecting best-fit models of protein evolution at ProtTest server (http://darwin.uvigo.es/software/prottest_server.html) (Abascal et al., 2005). The optimal setting for maximum-likelihood (ML) analysis was obtained as AIC: LG + I + G + F and the dendrogram was created in PhyML 3.0 using the appropriate substitution mode (Guindon et al., 2010). The starting tree was a BIO-NJ tree and the type of tree improvement was subtree pruning and regrafting (SPR) (Hordijk and Gascuel, 2005). The approximate likelihood ratio test (aLRT) with a Shimodaira–Hasegawa–like (SH-like) procedure (Anisimova and Gascuel, 2006) was used to calculate branch support values. The resulting tree was drawn by FigTree (version 1.3.1) (http://tree.bio.ed.ac.uk/software/figtree/) with the mid-pointed rooting.

Peptide mass fingerprinting (PMF)

Protein preparations were obtained by the virus purification method from virus-infected strain W1075 and isogenic virus-cured strain W1075-VF1. After confirming the presence of virus particles in the fraction from W1075, protein samples were analyzed by peptide mass fingerprinting in accordance with the protocol recommended by the manufacturer (Bruker Daltonics). Proteins were electrophoresed in a preparative SDS-polyacrylamide (10%) gel. Coomassie Brilliant Blue-stained proteins were recovered from the gel, digested with trypsin and subjected to PMF and subsequent MS/MS analyses, using MALDI-TOF/MS/MS (Bruker Daltonics) based on the method of Charoenpanich et al. (2006). The data were analyzed using Mascot software (Matrix Sciences) and a database containing the deduced amino acid sequences encoded by RnQV1 dsRNA1 to dsRNA4. Search results with significant MOWSE scores were taken into consideration.

Supplementary materials related to this article can be found online at doi:10.1016/j.virol.2012.01.013.

Acknowledgments

The authors are grateful to Yomogi Inc. (to NS) and the Program for Promotion of Basic and Applied Researches for Innovations in Bio-Oriented Industry (to SK, AS, and HK) for financial support during this study. We also thank Dr Said A. Ghabrial for the generous gift of *H. victoriae* fungal strains and fruitful discussion.

References

Abascal, F., Zardoya, R., Posada, D., 2005. ProtTest: selection of best-fit models of protein evolution. Bioinformatics 21, 2104–2105.

Aimi, T., Kano, S., Yotsutani, Y., Morinaga, T., 2002. Telomeric fingerprinting of the white root rot fungus, *Rosellinia necatrix*: a useful tool for strain identification. FEMS Microbiol. Lett. 217, 95–101.

Al Rwahnih, M., Daubert, S., Urbez-Torres, J.R., Cordero, F., Rowhani, A., 2011. Deep sequencing evidence from single grapevine plants reveals a virome dominated by mycoviruses. Arch. Virol. 156, 397–403.

Altschul, S.F., Madden, T.L., Schaffer, A.A., Zhang, J., Zhang, Z., Miller, W., Lipman, D.J., 1997. Gapped BLAST and PSI-BLAST: a new generation of protein database search programs. Nucleic Acids Res. 25, 3389–3402.
Anisimova, M., Gascuel, O., 2006. Approximate likelihood-ratio test for branches: a fast, accurate, and powerful alternative. Syst. Biol. 55, 539–552.
Aoki, N., Moriyama, H., Kodama, M., Arie, T., Teraoka, T., Fukuhara, T., 2009. A novel mycovirus associated with four double-stranded RNAs affects host fungal growth in *Alternaria alternata*. Virus Res. 140, 179–187.
Arakawa, M., Nakamura, H., Uetake, Y., Matsumoto, N., 2002. Presence and distribution of double-stranded RNA elements in the white root rot fungus *Rosellinia necatrix*. Mycoscience 43, 21–26.
Asamizu, T., Summers, D., Motika, M.B., Anzola, J.V., Nuss, D.L., 1985. Molecular cloning and characterization of the genome of wound tumor virus: a tumor-inducing plant reovirus. Virology 144, 398–409.
Cai, G., Myers, K., Hillman, B.I., Fry, W.E., 2009. A novel virus of the late blight pathogen, *Phytophthora infestans*, with two RNA segments and a supergroup 1 RNA-dependent RNA polymerase. Virology 392, 52–61.
Caston, J.R., Ghabrial, S.A., Jiang, D., Rivas, G., Alfonso, C., Roca, R., Luque, D., Carrascosa, J.L., 2003. Three-dimensional structure of penicillium chrysogenum virus: a double-stranded RNA virus with a genuine T=1 capsid. J. Mol. Biol. 331, 417–431.
Charoenpanich, J., Tani, A., Moriwaki, N., Kimbara, K., Kawai, F., 2006. Dual regulation of a polyethylene glycol degradative operon by AraC-type and GalR-type regulators in *Sphingopyxis macrogoltabida* strain 103. Microbiology 152, 3025–3034.
Chiba, S., Salaipeth, L., Lin, Y.H., Sasaki, A., Kanematsu, S., Suzuki, N., 2009. A novel bipartite double-stranded RNA mycovirus from the white root rot fungus *Rosellinia necatrix*: molecular and biological characterization, taxonomic considerations, and potential for biological control. J. Virol. 83, 12801–12812.
Chiba, S., Kondo, H., Tani, A., Saisho, D., Sakamoto, W., Kanematsu, S., Suzuki, N., 2011. Widespread endogenization of genome sequences of non-retroviral RNA viruses into plant genomes. PLoS Pathog. 7 (7), e1002146.
Covelli, L., Coutts, R.H., Di Serio, F., Citir, A., Acikgoz, S., Hernandez, C., Ragozzino, A., Flores, R., 2004. Cherry chlorotic rusty spot and Amasya cherry diseases are associated with a complex pattern of mycoviral-like double-stranded RNAs. I. Characterization of a new species in the genus *Chrysovirus*. J. Gen. Virol. 85, 3389–3397.
Faruk, M.I., Eusebio-Cope, A., Suzuki, N., 2008. A host factor involved in hypovirus symptom expression in the chestnut blight fungus, *Cryphonectria parasitica*. J. Virol. 82, 740–754.
Finn, R.D., Tate, J., Mistry, J., Coggill, P.C., Sammut, S.J., Hotz, H.R., Ceric, G., Forslund, K., Eddy, S.R., Sonnhammer, E.L., Bateman, A., 2008. The Pfam protein families database. Nucleic Acids Res. 36 (Database issue), D281–D288.
Ghabrial, S., 2008. Chrysoviruses. 3rd ed. In: Mahy, B.W.J., Van Regenmortel, M.H.V. (Eds.), Encyclopedia of Virology, Vol. 2. Elsevier, Oxford, pp. 284–291.
Ghabrial, S., Suzuki, N., 2009. Viruses of plant pathogenic fungi. Annu. Rev. Phytopathol. 47, 353–384.
Ghabrial, S.A., Soldevila, A.I., Havens, W.M., 2002. Molecular genetics of the viruses infecting the plant pathogenic fungus *Helminthosporium victoriae*. In: Tavantzis, S. (Ed.), Molecular biology of double-stranded RNA: concepts and applications in agriculture, forestry and medicine. CRC Press, Boca Raton, pp. 213–236.
Guindon, S., Dufayard, J.F., Lefort, V., Anisimova, M., Hordijk, W., Gascuel, O., 2010. New algorithms and methods to estimate maximum-likelihood phylogenies: assessing the performance of PhyML 3.0. Syst. Biol. 59 (3), 307–321.
Hillman, B.I., Suzuki, N., 2004. Viruses of the chestnut blight fungus, *Cryphonectria parasitica*. Advances in Virus Research, Vol. 63, Vol. 63. Elsevier Academic Press Inc., San Diego, pp. 423–472.
Hillman, B.I., Supyani, S., Kondo, H., Suzuki, N., 2004. A reovirus of the fungus *Cryphonectria parasitica* that is infectious as particles and related to the *Coltivirus* genus of animal pathogens. J. Virol. 78, 892–898.
Hordijk, W., Gascuel, O., 2005. Improving the efficiency of SPR moves in phylogenetic tree search methods based on maximum likelihood. Bioinformatics 21, 4338–4347.
Huang, S., Ghabrial, S.A., 1996. Organization and expression of the double-stranded RNA genome of *Helminthosporium victoriae 190S virus*, a totivirus infecting a plant pathogenic filamentous fungus. Proc. Natl. Acad. Sci. U. S. A. 93, 12541–12546.
Ikeda, K., Nakamura, H., Arakawa, M., Matsumoto, N., 2004. Diversity and vertical transmission of double-stranded RNA elements in root rot pathogens of trees, *Helicobasidium mompa* and *Rosellinia necatrix*. Mycol. Res. 108, 626–634.
Jamal, A., Bignell, E.M., Coutts, R.H., 2010. Complete nucleotide sequences of four dsRNAs associated with a new chrysovirus infecting *Aspergillus fumigatus*. Virus Res. 153, 64–70.
Jiang, D., Ghabrial, S.A., 2004. Molecular characterization of *Penicillium chrysogenum* virus: reconsideration of the taxonomy of the genus *Chrysovirus*. J. Gen. Virol. 85, 2111–2121.
Kanematsu, S., Arakawa, M., Oikawa, Y., Onoue, M., Osaki, H., Nakamura, H., Ikeda, K., Kuga-Uetake, Y., Nitta, H., Sasaki, A., Suzaki, K., Yoshida, K., Matsumoto, N., 2004. A reovirus causes hypovirulence of *Rosellinia necatrix*. Phytopathology 94, 561–568.
Katoh, K., Toh, H., 2008. Recent developments in the MAFFT multiple sequence alignment program. Brief. Bioinform. 9, 286–298.
Kondo, H., Maeda, T., Shirako, Y., Tamada, T., 2006. Orchid fleck virus is a rhabdovirus with an unusual bipartite genome. J. Gen. Virol. 87, 2413–2421.
Kozak, M., 1989. The scanning model for translation: an update. J. Cell Biol. 108, 229–241.
Kozlakidis, Z., Covelli, L., Di Serio, F., Citir, A., Acikgoz, S., Hernandez, C., Ragozzino, A., Flores, R., Coutts, R.H., 2006. Molecular characterization of the largest mycoviral-like double-stranded RNAs associated with Amasya cherry disease, a disease of presumed fungal aetiology. J. Gen. Virol. 87, 3113–3117.
Liu, H., Fu, Y., Jiang, D., Li, G., Xie, J., Peng, Y., Yi, X., Ghabrial, S.A., 2009. A novel mycovirus that is related to the human pathogen hepatitis E virus and rubi-like viruses. J. Virol. 83, 1981–1991.
Nakamura, H., Ikeda, K., Arakawa, M., Matsumoto, N., 2002. Conidioma production of the white rooto rot fungus in axenic culture under near-ultravioret light radiation. Mycoscience 43, 251–254.
Nuss, D.L., 2005. Hypovirulence: mycoviruses at the fungal–plant interface. Nat. Rev. Microbiol. 3, 632–642.
Nuss, D.L., 2011. Mycoviruses, RNA silencing, and viral RNA recombination. Adv. Virus Res. 80, 25–48.
Oh, C.S., Hillman, B.I., 1995. Genome organization of a partitivirus from the filamentous ascomycete *Atkinsonella hypoxylon*. J. Gen. Virol. 76, 1461–1470.
Pearson, M.N., Beever, R.E., Boine, B., Arthur, K., 2009. Mycoviruses of filamentous fungi and their relevance to plant pathology. Mol. Plant Pathol. 10, 115–128.
Pliego, C., Kanematsu, S., Ruano-Rosa, D., de Vicente, A., Lopez-Herrera, C., Cazorla, F.M., Ramos, C., 2009. GFP sheds light on the infection process of avocado roots by *Rosellinia necatrix*. Fungal Genet. Biol. 46, 137–145.
Prilusky, J., Felder, C.E., Zeev-Ben-Mordehai, T., Rydberg, E.H., Man, O., Beckmann, J.S., Silman, I., Sussman, J.L., 2005. FoldIndex: a simple tool to predict whether a given protein sequence is intrinsically unfolded. Bioinformatics 21, 3435–3438.
Sanderlin, R.S., Ghabrial, S.A., 1978. Physicochemical properties of two distinct types of virus-like particles from *Helminthosporium victoriae*. Virology 87, 142–151.
Sasaki, A., Miyanishi, M., Ozaki, K., Onoue, M., Yoshida, K., 2005. Molecular characterization of a partitivirus from the plant pathogenic ascomycete *Rosellinia necatrix*. Arch. Virol. 150, 1069–1083.
Sasaki, A., Kanematsu, S., Onoue, M., Oikawa, Y., Nakamura, H., Yoshida, K., 2007. Artificial infection of *Rosellinia necatrix* with purified viral particles of a member of the genus *Mycoreovirus* reveals its uneven distribution in single colonies. Phytopathology 97, 278–286.
Segers, G.C., Zhang, X., Deng, F., Sun, Q., Nuss, D.L., 2007. Evidence that RNA silencing functions as an antiviral defense mechanism in fungi. Proc. Natl. Acad. Sci. U. S. A. 104, 12902–12906.
Stuart, K.D., Weeks, R., Guilbride, L., Myler, P.J., 1992. Molecular organization of Leishmania RNA virus 1. Proc. Natl. Acad. Sci. U. S. A. 89, 8596–8600.
Sun, L., Suzuki, N., 2008. Intragenic rearrangements of a mycoreovirus induced by the multifunctional protein p29 encoded by the prototypic hypovirus CHV1-EP713. RNA 14, 2557–2571.
Sun, L., Nuss, D.L., Suzuki, N., 2006. Synergism between a mycoreovirus and a hypovirus mediated by the papain-like protease p29 of the prototypic hypovirus CHV1-EP713. J. Gen. Virol. 87, 3703–3714.
Suzuki, N., Maruyama, K., Moriyama, M., Nuss, D.L., 2003. Hypovirus papain-like protease p29 functions in trans to enhance viral double-stranded RNA accumulation and vertical transmission. J. Virol. 77, 11697–11707.
Suzuki, N., Supyani, S., Maruyama, K., Hillman, B.I., 2004. Complete genome sequence of Mycoreovirus-1/Cp9B21, a member of a novel genus within the family *Reoviridae*, isolated from the chestnut blight fungus *Cryphonectria parasitica*. J. Gen. Virol. 85, 3437–3448.
Tamura, K., Dudley, J., Nei, M., Kumar, S., 2007. MEGA4: Molecular Evolutionary Genetics Analysis (MEGA) software version 4.0. Mol. Biol. Evol. 24 (8), 1596–1599.
Tavantzis, S., 2008. Partitiviruses of fungi, In: Mahy, B.W.J., Van Regenmortel, M.H.V. (Eds.), Encyclopedia of Virology, 3rd ed. Elsevier, Oxford, pp. 63–68.
Tuomivirta, T.T., Hantula, J., 2003. Gremmeniella abietina mitochondrial RNA virus S1 is phylogenetically related to the members of the genus *Mitovirus*. Arch. Virol. 148, 2429–2436.
Urayama, S., Kato, S., Suzuki, Y., Aoki, N., Le, M.T., Arie, T., Teraoka, T., Fukuhara, T., Moriyama, H., 2010. Mycoviruses related to chrysovirus affect vegetative growth in the rice blast fungus *Magnaporthe oryzae*. J. Gen. Virol. 91, 3085–3094.
Wei, C.Z., Osaki, H., Iwanami, T., Matsumoto, N., Ohtsu, Y., 2004. Complete nucleotide sequences of genome segments 1 and 3 of Rosellinia anti-rot virus in the family *Reoviridae*. Arch. Virol. 149, 773–777.
Yaegashi, H., Sawahata, T., Ito, T., Kanematsu, S., 2010. A novel colony-print immunoassay reveals differential patterns of distribution and horizontal transmission of four unrelated mycoviruses in *Rosellinia necatrix*. Virology 409, 280–289.